Kinetic and Mechanistic Study of the Self Reaction of $CH_3OCH_2O_2$ Radicals at Room Temperature

Michael E. Jenkin* and Garry D. Hayman

Chemical Kinetics Section, AEA Consultancy Services, B551, Harwell Laboratory, Oxfordshire OX11 0RA, U.K.

Timothy J. Wallington,* Michael D. Hurley, and James C. Ball

Research Staff, SRL-3083, Ford Motor Company, P.O. Box 2053, Dearborn, Michigan 48121

Ole John Nielsen* and Thomas Ellermann

Section for Chemical Reactivity, Risø National Laboratory, DK-4000 Roskilde, Denmark

*Received: June 24, 1993; In Final Form: August 23, 1993**

The UV absorption spectrum and kinetics of the self reaction of $CH_3OCH_2O_2$ at 298 K have been studied using both the modulated photolysis of $Cl_2/CH_3OCH_3/O_2/N_2$ mixtures and the pulse radiolysis of $SF_6/CH_3OCH_3/O_2$ mixtures. The spectrum, characterized in the range 200–290 nm, is in good agreement with the single published determination.[8] The observed second-order removal kinetics of $CH_3OCH_2O_2$, k_{5obs}, were found to be sensitive to both the variation of total pressure (17–760 Torr) and the composition of the reaction mixtures: $2CH_3OCH_2O_2 \rightarrow 2CH_3OCH_2O + O_2$ (5a); $\rightarrow CH_3OCHO + CH_3OCH_2OH + O_2$ (5b). The kinetic studies and a detailed product investigation using long path length FTIR spectroscopy (T = 295 K; $Cl_2/CH_3OCH_3/O_2/N_2$ system) provide evidence to support a mechanism involving the rapid thermal decomposition of CH_3OCH_2O by H atom ejection occurring in competition with the reaction with O_2: CH_3OCH_2O (+M) $\rightarrow CH_3OCHO + H$ (+M) (6); $CH_3OCH_2O + O_2 \rightarrow CH_3OCHO + HO_2$ (4). The complications in the measured values of k_{5obs} in the present studies, and those reported previously,[8] are believed to occur as a direct result of formation of H atoms from reaction 6. Accordingly, a pressure-independent value of $k_5 = (2.1 \pm 0.3) \times 10^{-12}$ cm^3 molecule^{-1} s^{-1} is derived for the elementary rate coefficient at 298 K, with identical values of the branching ratio $\alpha = k_{5a}/k_5 = 0.7 \pm 0.1$ determined independently from the FTIR product studies and the modulated photolysis experiments. As part of this work, the rate coefficient for the reaction of Cl atoms with CH_3OCH_2Cl was found to be $(2.9 \pm 0.2) \times 10^{-11}$ cm^3 molecule^{-1} s^{-1}.

1. Introduction

The role played by organic peroxy radicals (RO_2) in the tropospheric oxidation of volatile organic compounds is well documented.[1-3] The reactions of RO_2 with NO, NO_2, and HO_2 are key processes in the mechanisms describing the generation of secondary oxidants such as O_3, and a variety of carbonyl compounds, peroxides, and organic nitrogen oxide species. The self reactions of RO_2, although of limited importance under tropospheric conditions, are usually a major complication in laboratory studies and often needed to be characterized thoroughly before reliable data can be obtained on the tropospherically important reactions.

In recent years, significant progress has been made in defining structure–reactivity relationships for both the kinetics and branching ratios of reactions of RO_2 radicals,[3,4] and the influence of a variety of substituent functional groups on their reactivity can be assessed. There is, however, only limited information available on the effect of an "alkoxy" group adjacent to a peroxy radical center. The simplest α-alkoxy alkyl peroxy radical (which are derived from the oxidation of ethers in general) is the methoxy methyl peroxy radical ($CH_3OCH_2O_2$), formed in the atmosphere from the OH radical initiated oxidation of dimethyl ether:

$$OH + CH_3OCH_3 \rightarrow CH_3OCH_2 + H_2O \quad (1)$$

$$CH_3OCH_2 + O_2\ (+M) \rightarrow CH_3OCH_2O_2\ (+M) \quad (2)$$

In their FTIR product study, Japar et al.[5] established that methyl formate (CH_3OCHO) is produced almost quantitatively from the Cl atom initiated oxidation of CH_3OCH_3 in the presence of NO. By analogy with other organic peroxy radicals,[3,4] this was attributed to the following reaction sequence:

$$CH_3OCH_2O_2 + NO \rightarrow CH_3OCH_2O + NO_2 \quad (3)$$

$$CH_3OCH_2O + O_2 \rightarrow CH_3OCHO + HO_2 \quad (4)$$

The observed product, CH_3OCHO, was thus believed to be generated from the reaction of the methoxy methoxy radical intermediate (CH_3OCH_2O) with O_2, i.e. analogous to the reaction commonly observed for simple alkoxy radicals possessing C–H bonds α to the radical center.[6] In the absence of NO, CH_3OCHO has also been detected as a major product[7] using FTIR spectroscopy, although the yield was not quantified. Under these conditions, $CH_3OCH_2O_2$ is removed by its self reaction (eq 5), which is believed to have the following major channels:[3,4]

$$2CH_3OCH_2O_2 \rightarrow 2CH_3OCH_2O + O_2 \quad (5a)$$

$$\rightarrow CH_3OCHO + CH_3OCH_2OH + O_2 \quad (5b)$$

Consequently, CH_3OCHO may be formed either directly from channel 5b or from the subsequent chemistry of CH_3OCH_2O produced in channel 5a.

In the single published kinetic study of $CH_3OCH_2O_2$, Dagaut et al.[8] generated the radical by flash photolysis of Cl_2 in the presence of CH_3OCH_3 and O_2, with detection by UV absorption spectroscopy. The UV spectrum of $CH_3OCH_2O_2$ was found to be typical of an organic peroxy radical (i.e. broad and unstructured), with a maximum absorption cross section of 4.06×10^{-18} cm^2 molecule^{-1} at 230 nm. In contrast, derived values of k_5

* Abstract published in *Advance ACS Abstracts*, October 1, 1993.

0022-3654/93/2097-11712$04.00/0

displayed unusual dependences on both temperature and pressure. At 298 K, k_5 apparently varied between 7×10^{-13} cm^3 molecule^{-1} s^{-1} at 25 Torr and 2.4×10^{-12} cm^3 molecule^{-1} s^{-1} at 800 Torr, an unexpected result, since all other RO_2 radical self reactions studied to date have pressure-independent rate coefficients over comparable ranges.[3,4] In the absence of mechanistic information, it was not clear whether this was due to a pressure dependence of the elementary rate coefficient or as a result of unforeseen secondary chemistry.

In this paper, a detailed investigation of the kinetics and products of reaction 5 at temperatures near 298 K is presented. Although under some conditions the observed kinetics were found to be sensitive to variation of pressure, the apparent rate coefficient (k_{5obs}) could also be varied by changing the composition of the reaction mixtures. As a result of this work, we are able to conclude that the elementary rate coefficient (k_5) is insensitive to variation of pressure. Evidence is presented which supports a mechanism involving the rapid thermal decomposition of the CH_3OCH_2O radical (formed in reaction 5a) by H atom ejection:

$$CH_3OCH_2O\ (+M) \rightarrow CH_3OCHO + H\ (+M) \quad (6)$$

The complications in the measured rate coefficient k_{5obs} are believed to occur as a direct result of the formation of H atoms from reaction 6.

2. Experimental Section

The kinetic experiments were carried out using both the molecular modulation (AEA CS, Harwell) and pulse radiolysis (Risø National Laboratory) techniques. The product studies were performed using long path length Fourier transform infrared (FTIR) spectroscopy (Ford Motor Company). Complete descriptions of these experimental systems have been given previously,[7,9-12] so they are only discussed briefly in the present paper.

2.1. Molecular Modulation Experiments. Experiments were performed at 298 K in a temperature-regulated, cylindrical quartz reaction vessel (volume 1.2 dm^3; length 120 cm). $CH_3OCH_2O_2$ was generated by the intermittent photolysis of Cl_2 (2.5–55 $\times$ 10^{15} molecule cm^{-3}) in the presence of CH_3OCH_3 (1.2–2.7 $\times$ 10^{17} molecule cm^{-3}) and O_2 (6.1–770 $\times$ 10^{16} molecule cm^{-3}):

$$Cl_2 + h\nu \rightarrow Cl + Cl \quad (7)$$

$$Cl + CH_3OCH_3 \rightarrow CH_3OCH_2 + HCl \quad (8)$$

$$CH_3OCH_2 + O_2\ (+M) \rightarrow CH_3OCH_2O_2\ (+M) \quad (2)$$

Experiments were carried out as a function of total pressure over the range 17–760 Torr, with N_2 providing the balance of the gas pressure. Photolysis of Cl_2 was achieved using up to five fluorescent black lights (Sankyo Denki FL405), emitting over the wavelength range 310–400 nm. Reaction mixtures were monitored using a collimated beam from a deuterium lamp, which was focused onto the slit of a 0.75-m monochromator (Spex 1700), followed by detection on a photomultiplier (EMI, 9783B). The modulated absorption signals due to the production and removal of $CH_3OCH_2O_2$ (typically 10^{-3}) were accumulated and averaged in the manner described previously.[7,9]

Kinetic measurements were made using flowing gas mixtures to minimize the accumulation of reaction products. The residence time in the vessel was ca. 15 s. The flows of the constituent gases were either regulated using mass flow controllers (MKS, Type 261) or monitored using calibrated rotameters. The total pressure in the reaction vessel was measured using a capacitance manometer (MKS Baratron, Model 170M-6B), allowing calculation of the partial pressures of the component gases. The concentration of Cl_2 was also determined directly by conventional absorption spectroscopy ($\sigma_{330nm} = 2.56 \times 10^{-19}$ cm^2 molecule^{-1}).[13] N_2 (Air Products, high purity), O_2 (BOC, breathing grade), CH_3OCH_3 (Aldrich), and Cl_2 (Union Carbide, 5% in high-purity N_2) were used as received.

2.2. Pulse Radiolysis Experiments. $CH_3OCH_2O_2$ radicals were generated by the irradiation of $SF_6/O_2/CH_3OCH_3$ mixtures in a 1-dm^3 stainless steel reactor with a single 30-ns pulse of 2-MeV electrons from a Febetron 705B field emission accelerator as follows:

$$SF_6 + 2\text{-MeV } e^- \rightarrow F + \text{products} \quad (9)$$

$$F + CH_3OCH_3 \rightarrow CH_3OCH_2 + HF \quad (10)$$

$$CH_3OCH_2 + O_2\ (+M) \rightarrow CH_3OCH_2O_2\ (+M) \quad (2)$$

Transient absorptions due to $CH_3OCH_2O_2$ (typically 10^{-1}) were monitored using the output of a pulsed 150-W Xenon arc lamp, coupled to an internally mounted White optical arrangement allowing variation of the path length in the range 40–160 cm. Spectral features were analyzed using a 1-m grating spectrograph (Hilger & Watts), with the light intensity monitored by a photomultiplier (Hamamatsu) and digitized using a transient recorder (Biomation 8100). Measurements of the UV spectrum of $CH_3OCH_2O_2$ were made by observing the maximum in the transient UV absorption at short times (10–40 μs) after the radiation pulse. Using longer time scales (0.4–4.0 ms), the subsequent decay of the absorption was monitored to obtain the kinetic information.

Gas mixtures were prepared by adding one component at a time and measuring the corresponding partial pressure using an absolute membrane nanometer (MKS Baratron 170) with a resolution of 10^{-2} Torr. Experiments were carried out at 298 K over the pressure range 75–750 Torr, with the following reagent concentrations: O_2, 8.6×10^{17} molecule cm^{-3}; CH_3OCH_3, 2.4–22×10^{16} molecule cm^{-3}; SF_6, varied to make up the desired total pressure. Ultra high purity SF_6 (99.9%, Gerling and Holtz), O_2 (L'Air Liquide), and CH_3OCH_3 (99.9%, Union Carbide Industrial Gases) were used as received.

2.3. Long Path Length FTIR Experiments. All experiments were performed in a 140-dm^3 Pyrex reactor, surrounded by 22 fluorescent black lamps (GE F15T8-BL). $CH_3OCH_2O_2$ radicals were generated by the photolysis of Cl_2 in the presence of CH_3OCH_3 in O_2/N_2 mixtures (reaction sequence (7), (8), and (2)) at total pressures in the range 10–700 Torr at 295 $\pm$ 2 K. The loss of CH_3OCH_3 and the formation of products were monitored by FTIR spectroscopy using an infrared path length of 26 m and a resolution of 0.25 cm^{-1}. Infrared spectra were derived from 32–128 co-added interferograms. Reference spectra were obtained by expanding known volumes of the reference material into the long path length cell at appropriate pressures of air diluent. Products were identified and quantified by fitting reference spectra of the pure compounds obtained at the appropriate total pressures to the observed product spectra using integrated absorption features over the following wavelength ranges (in cm^{-1}): CH_3OCHO, 1000–1100; methoxy methyl hydroperoxide (CH_3OCH_2OOH), 775–850 and 1700–1750; chloromethyl methyl ether (CH_3OCH_2Cl), 650–850 and 1200–1300; HCHO, 1700–1800; HCOOH, 1050–1150; and CO, 2050–2250. CH_3OCH_2OOH was prepared by the ozonolysis of vinyl chloride (99.9% purity) in methanol (>99.9% purity) at 195 K[14] and was purified by vacuum distillation. No observable impurities were detected by FTIR spectroscopic analysis of the purified hydroperoxide sample. The other species were obtained from commercial sources at the highest available purity. The initial CH_3OCH_3 concentrations used were in the range $(9.1–10.8) \times 10^{14}$ molecule cm^{-3}. Further details regarding the experimental conditions are given in section 3.2.

3. Results

3.1. Self Reaction Kinetics and UV Absorption Spectrum of $CH_3OCH_2O_2$. *Molecular Modulation Experiments.* $CH_3OCH_2O_2$ radicals produced by the modulated photolysis of $Cl_2/CH_3OCH_3/O_2$ mixtures were detected by UV absorption spectroscopy in the wavelength range 200–290 nm. Typical modulated

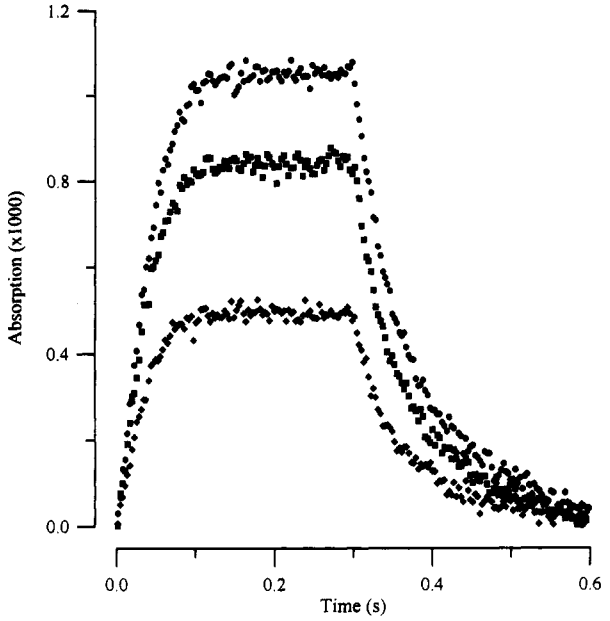

Figure 1. Absorption waveforms obtained at 220 nm (●), 240 nm (■), and 260 nm (◆) from the modulated photolysis of $Cl_2/CH_3OCH_3/O_2/N_2$ at 298 K and 760 Torr ($[O_2]/[Cl_2]$ = 850).

absorption waveforms are shown in Figure 1. Although experiments were carried out under a variety of conditions (as discussed below), the observed behavior of $CH_3OCH_2O_2$ was always well described by a second-order kinetic analysis, indicative of removal via the self reaction:

$$2CH_3OCH_2O_2 \rightarrow 2CH_3OCH_2O + O_2 \qquad (5a)$$

$$\rightarrow CH_3OCHO + CH_3OCH_2OH + O_2 \qquad (5b)$$

Using the methods of analysis described in previous papers,[7,9] values of k_{5obs}/σ were derived for each set of conditions (k_{5obs} is the observed or apparent second-order rate coefficient). Provided the radical production rate (=$2k_7[Cl_2]$) is known, both k_{5obs} and σ can be determined. To enable this, the first-order decay constant for Cl_2 (k_7) was measured in independent experiments in which static mixtures comprised of Cl_2, H_2, and O_2 were photolysed and the decay of Cl_2 was monitored. A value of $k_7 = (4.4 \pm 0.1) \times 10^{-3}$ s^{-1} for five black lights was obtained.

In an initial series of experiments, the effect of varying pressure in the range 17–760 Torr on the observed behavior of $CH_3OCH_2O_2$ (monitored at 240 nm) was investigated. For these experiments, $[O_2]$ was kept constant at 3×10^{17} molecule cm^{-3}, with $[Cl_2]$ in the narrow range $2.5–3.5 \times 10^{15}$ molecule cm^{-3}. At low pressures, k_{5obs} decreased significantly, in qualitative agreement with the observations of Dagaut et al.[8] As shown in Figure 2, however, the absolute values of k_{5obs} and the shape of the apparent falloff measured in the present study are significantly different from those observed in the study of Dagaut et al.[8] Although the O_2 concentration used in both studies is similar, the concentrations of Cl_2 used by Dagaut et al. were up to an order of magnitude greater. The effect of variation of both $[Cl_2]$ and $[O_2]$ was investigated, therefore, in an extensive series of experiments performed at a fixed pressure (760 Torr), and it was found that the value of k_{5obs} was influenced by varying the concentration of either Cl_2 or O_2. Figure 3 shows the dependence of k_{5obs} on the concentration ratio $[O_2]/[Cl_2]$. At high-concentration ratios (ca. 1000), values of $k_{5obs} \approx 3.5 \times 10^{-12}$ cm^3 molecule^{-1} s^{-1} were obtained, whereas at low ratios (ca. 1), values of $k_{5obs} < 10^{-12}$ cm^3 molecule^{-1} s^{-1} were observed. Clearly, therefore, the sensitivity of k_{5obs} to the experimental conditions arises from complications in the secondary chemistry and not simply from a complex dependence of the elementary rate coefficient on pressure, as postulated previously.[8] More specifically, the dependence on the

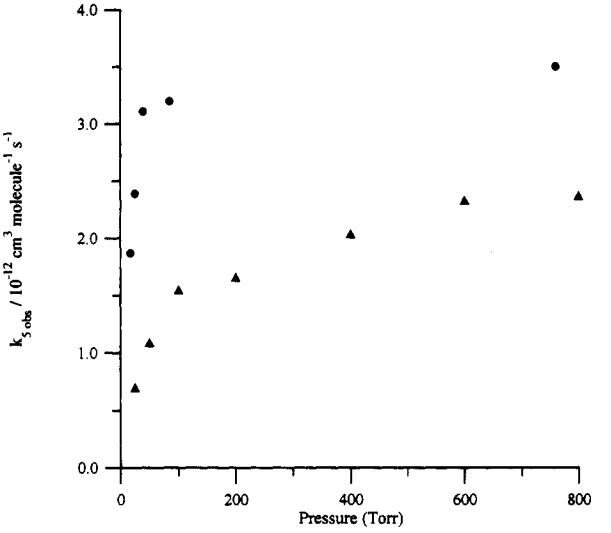

Figure 2. Values of the apparent rate coefficient, k_{5obs}, measured as a function of pressure at 298 K using a $Cl_2/CH_3OCH_3/O_2/N_2$ system in the present study (●) and in the study of Dagaut et al.[8] (▲) (see discussion in text).

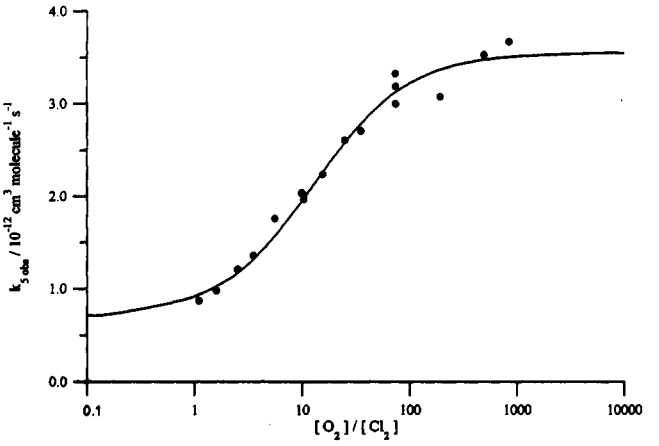

Figure 3. Values of the apparent rate coefficient, k_{5obs}, measured as a function of the concentration ratio $[O_2]/[Cl_2]$ at 760 Torr and 298 K. Line is curve computed on the basis of the linear regression displayed in Figure 5.

ratio $[O_2]/[Cl_2]$ indicates a direct competition between reactions of a short-lived intermediate with O_2 and with Cl_2. In explaining this effect, and identifying the key intermediate (referred to as "X" in the following discussion), several criteria must be fulfilled: (a) $CH_3OCH_2O_2$ displayed second-order kinetic behavior under all experimental conditions. Consequently, X cannot be $CH_3OCH_2O_2$ itself. (b) The observed production efficiency of $CH_3OCH_2O_2$ from Cl_2 photolysis was independent of experimental conditions (i.e. the initial production of $CH_3OCH_2O_2$ was not inhibited). This indicates that X must be a short-lived species generated from reaction of $CH_3OCH_2O_2$, i.e. probably as a result of reaction channel 5a. (c) Either the reaction of X with O_2 leads to further removal of $CH_3OCH_2O_2$, or the reaction of X with Cl_2 leads to regeneration of $CH_3OCH_2O_2$, or both. (d) For the observed pressure effect to be consistent with the observed $[O_2]/[Cl_2]$ effect, the reaction of X with O_2 must become less competitive as the pressure is lowered, indicating that it is an association reaction. Since at low values of $[O_2]/[Cl_2]$, a pressure effect can even be observed at high pressures (e.g. the data of Dagaut et al. displayed in Figure 2), the reaction of X with O_2 must be well below its high-pressure limit, indicating that X is a small species.

A plausible explanation for all the experimental observations may be forwarded, if it is assumed that CH_3OCH_2O formed in reaction channel 5a decomposes by ejection of an H atom in

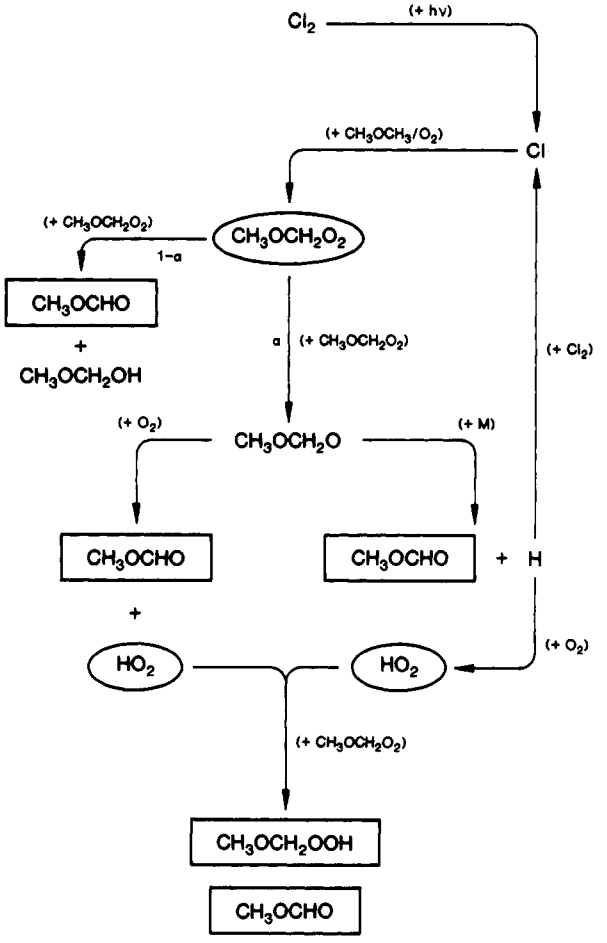

Figure 4. Schematic representation of the Cl atom initiated oxidation mechanism of CH_3OCH_3 at high pressure.

preference to reacting with O_2:

$$2CH_3OCH_2O_2 \rightarrow 2CH_3OCH_2O + O_2 \quad (5a)$$

$$CH_3OCH_2O\ (+M) \rightarrow CH_3OCHO + H\ (+M) \quad (6)$$

Other than H, it is difficult to identify a species which fulfills all the criteria outlined above for the key intermediate "X".

At high total pressures and $[O_2]$, the association reaction of H with O_2 is favored, leading to further removal of $CH_3OCH_2O_2$ as follows:

$$H + O_2\ (+M) \rightarrow HO_2\ (+M) \quad (11)$$

$$HO_2 + CH_3OCH_2O_2 \rightarrow \text{products} \quad (12)$$

As the total pressure is lowered, or the $[O_2]/[Cl_2]$ ratio is decreased, the pressure-independent reaction of H with Cl_2 becomes more competitive, leading to production of Cl and regeneration of $CH_3OCH_2O_2$:

$$H + Cl_2 \rightarrow HCl + Cl \quad (13)$$

$$Cl + CH_3OCH_3 \rightarrow CH_3OCH_2 + HCl \quad (8)$$

$$CH_3OCH_2 + O_2\ (+M) \rightarrow CH_3OCH_2O_2\ (+M) \quad (2)$$

According to this mechanism (shown schematically in Figure 4) and assuming reaction 12 is exclusive for HO_2, k_{5obs} should vary between $(1 + \alpha)k_5$ when reaction 11 dominates and $(1 - \alpha)k_5$ when reaction 13 dominates, where $\alpha = k_{5a}/k_5$. Furthermore, the complete dependence of k_{5obs} on $[O_2]$ and $[Cl_2]$ should be given by the expression

$$k_{5obs} = (1 + f\alpha)k_5$$

where the parameter $f = (k_{11}[O_2] - k_{13}[Cl_2])/(k_{11}[O_2] + k_{13}[Cl_2])$, taking values between −1.0 and +1.0. Figure 5 shows

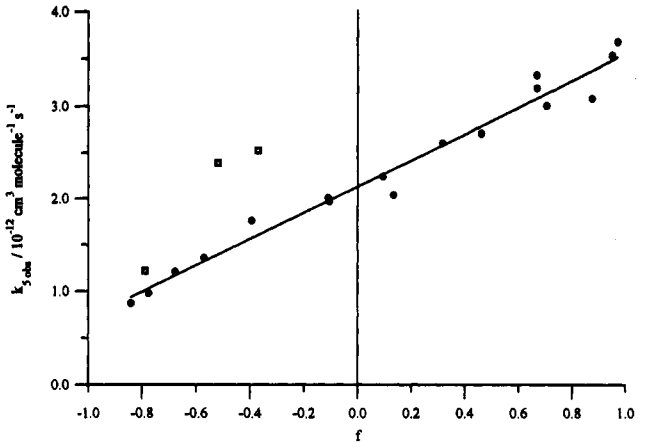

Figure 5. Values of the apparent rate coefficient, k_{5obs}, plotted as a function of the parameter f (see discussion in text): (●) data obtained at 760 Torr; (□) data obtained at 25 Torr. Line is linear regression of 760-Torr data.

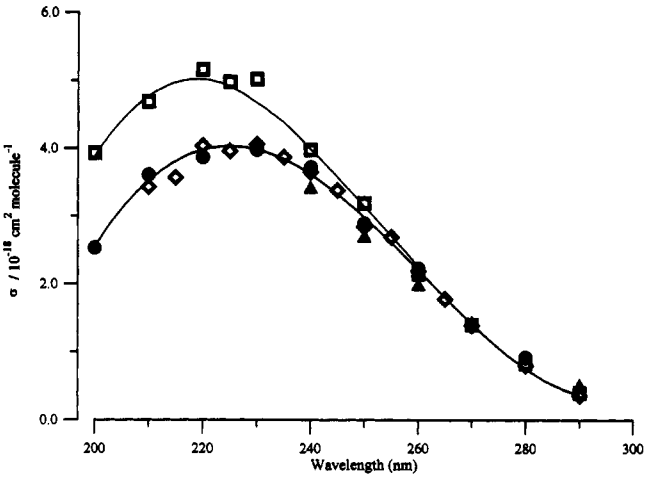

Figure 6. Absorption spectra measured for $CH_3OCH_2O_2$ at 298 K: (●) molecular modulation experiments with $[O_2]/[Cl_2] = 1.1$ (lower line is fifth-order polynomial fit to data); (□) molecular modulation experiments with $[O_2]/[Cl_2] = 850$ (upper line obtained by adding HO_2 spectrum to lower line); (▲) pulse radiolysis experiments; (◇) data of Dagaut et al.

acorresponding plot of k_{5obs} vs f for the set of data displayed in Figure 3 (total pressure 760 Torr), with f calculated using recommended values of k_{11} and k_{13}.[15] The linearity of this plot is consistent with the posulated mechanism and also allows determination of both k_5 and α from the slope and intercept (errors = $\pm 2\sigma$):

$$k_5 = (2.13 \pm 0.30) \times 10^{-12}\ cm^3\ molecule^{-1}\ s^{-1}$$

$$\alpha = 0.67 \pm 0.11$$

Further support for the mechanism presented above comes from the UV spectral measurements of $CH_3OCH_2O_2$. Experiments were performed in which the variation of the modulated absorption signal with wavelength was investigated at $[O_2]/[Cl_2]$ ratios of both 1.1 and 850. The derived absorption cross sections are presented in Figure 6, along with the data of Dagaut et al.,[8] obtained using the flash photolysis technique. The spectrum measured with $[O_2]/[Cl_2] = 1.1$ is in excellent agreement with the data of Dagaut et al., both in shape and magnitude. With $[O_2]/[Cl_2] = 850$, however, the data obtained at the short end of the wavelength range in the present study clearly lie above those measured with $[O_2]/[Cl_2] = 1.1$. This is consistent with the mechanism postulated above, since at high $[O_2]/[Cl_2]$, a contribution to the measured spectrum is made by a steady-state concentration of HO_2 formed from reaction 11. At low $[O_2]/[Cl_2]$, the formation of HO_2 is inhibited, since reaction 13 competes effectively with reaction 11. As can be seen in Figure 6, the difference between the two sets of data matches the HO_2 spectrum

extremely closely. Furthermore, these data suggest the steady-state concentration ratio $[HO_2]/[CH_3OCH_2O_2] \approx 0.3$ when reaction 11 dominates, which according to the postulated mechanism, should be equal to the expression $2\alpha k_5/k_{12}$. Thus, on the basis of the values of k_5 and α derived above, k_{12} is the order of 10^{-11} cm^3 molecule^{-1} s^{-1}, i.e. typical for reactions of larger organic peroxy radicals with HO_2.[3,4]

Since the reaction of H with O_2 (reaction 11) is strongly pressure dependent,[15] the apparent falloff in k_{5obs} at lower pressures observed by Dagaut et al.[8] and in the present experiments is also qualitatively explained by the proposed mechanism. However, on the basis of reported values of k_{11} as a function of pressure,[15] the present data suggest that the reduction in k_{5obs} with a decrease in pressure at approximately constant $[O_2]/[Cl_2]$ (Figure 2) is not as great as would be expected from the pressure dependence of the competition between reactions 11 and 13 for H. Clearly, the ejection of H from CH_3OCH_2O (reaction 6) will itself possess a pressure dependence, possibly allowing other reactions to become competitive for CH_3OCH_2O at low pressures. To provide more information, a series of experiments was performed at 25 Torr to investigate the effect of varying $[O_2]/[Cl_2]$ on the measured value of k_{5obs}. The results are shown as a function of the parameter f in Figure 5, along with those obtained at 760 Torr. For the 25-Torr experiments, $[Cl_2]$ was kept constant at $(3.0 \pm 0.5) \times 10^{15}$ molecule cm^{-3}, with $[O_2]$ varied in the range $1-6 \times 10^{17}$ molecule cm^{-3}. Although at the lowest $[O_2]$ ($f = -0.79$) the measured value of k_{5obs} is in reasonable agreement with those obtained at 760 Torr, the increase in k_{5obs} as $[O_2]$ (and therefore f) is raised is far more rapid than expected solely on the basis of the competition between reactions 11 and 13 for H. As a result, the dependence of k_{5obs} on f is no longer linear, with the $(1 + \alpha)k_5$ (i.e. maximum) value being approached at values of $f \ll 1$. These results give an indication that the reaction of CH_3OCH_2O with O_2 (reaction 4) is competing with reaction 6:

$$CH_3OCH_2O + O_2 \rightarrow CH_3OCHO + HO_2 \quad (4)$$

$$CH_3OCH_2O\ (+M) \rightarrow CH_3OCHO + H\ (+M) \quad (6)$$

Reaction 4 has the same overall effect as reaction 6 followed by reaction of H with O_2 (reaction 11) and therefore leads to additional removal of $CH_3OCH_2O_2$ by reaction 12. Consequently, the measured value of k_{5obs} at 25 Torr is not only influenced by the $[O_2]/[Cl_2]$ ratio but also by the absolute $[O_2]$.

Given that the competition between reactions 4 and 6 appears to occur at 25 Torr with $[O_2]$ in the range $1-6 \times 10^{17}$ molecule cm^{-3}, it is probable that the competition also exists at 760 Torr, but at much higher $[O_2]$ (probably $> 10^{18}$ molecule cm^{-3}) when both reactions are correspondingly more rapid. The effect of this competition on the data obtained at 760 Torr is not observable, however, because, under conditions when reaction 4 is able to compete with reaction 6, $[O_2]$ is sufficiently high that H reacts almost exclusively with O_2 and reactions 4 and 6 are essentially indistinguishable. At lower $[O_2]$ ($<10^{18}$ molecule cm^{-3}, corresponding to $f < 0.9$ in Figure 5) ejection of H is probably the sole fate of CH_3OCH_2O at 760 Torr.

Pulse Radiolysis Experiments. The radiolysis of $SF_6/CH_3OCH_3/O_2$ mixtures resulted in a rapid increase in UV absorption (230–290 nm), followed by a slower decay. Figure 7 shows a typical data profile obtained by monitoring the transient absorption at 260 nm, following radiolysis of a mixture containing 2.2×10^{17} molecule cm^{-3} CH_3OCH_3 and 8.6×10^{17} molecule cm^{-3} O_2, made up to a total pressure of 612 Torr with SF_6. The trace shown is the result of a single pulse, i.e. with no signal averaging. Control experiments were performed in which single components and mixtures of two of the three components were subjected to pulse radiolysis; no transient absorption was detected ($<10^{-2}$ absorbance units). The observed UV absorptions (e.g. Figure 7) are therefore ascribed to the formation of $CH_3OCH_2O_2$ radicals, and their subsequent removal initiated by reaction 5:

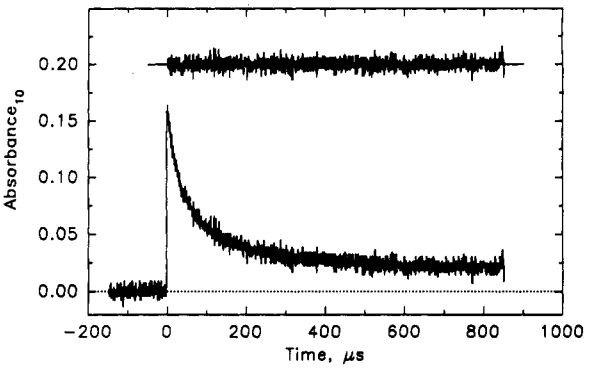

Figure 7. Transient decay profile obtained at 260 nm following the pulse radiolysis of $SF_6/CH_3OCH_3/O_2$ at 612 Torr and 298 K. The absorption path length was 40 cm.

$$2CH_3OCH_2O_2 \rightarrow 2CH_3OCH_2O + O_2 \quad (5a)$$

$$\rightarrow CH_3OCHO + CH_3OCH_2OH + O_2 \quad (5b)$$

An initial series of experiments was carried out to determine absolute absorption cross sections for $CH_3OCH_2O_2$. In order to do this, a calibration of the initial yield of F atoms resulting from the radiolysis of SF_6 was required. This was achieved by monitoring the transient absorption at 250 nm due to CH_3O_2 radicals produced from the radiolysis of $SF_6/CH_4/O_2$ mixtures.[16] Using an average recommended value of $\sigma_{250nm} = 4.01 \times 10^{-18}$ cm^2 molecule^{-1} for CH_3O_2,[3,4] the yield of F atoms at 750 Torr SF_6 and full irradiation dose was found to be $(3.12 \pm 0.33) \times 10^{15}$ molecule cm^{-3}. The quoted error includes an estimated uncertainty of $\pm 10\%$ in σ_{250nm} for CH_3O_2.

For accurate spectral measurements to be made, experiments must be performed under conditions where F atoms are converted stoichiometrically into $CH_3OCH_2O_2$ radicals by the reaction sequence (10) followed by (2):

$$F + CH_3OCH_3 \rightarrow CH_3OCH_2 + HF \quad (10)$$

$$CH_3OCH_2 + O_2\ (+M) \rightarrow CH_3OCH_2O_2\ (+M) \quad (2)$$

Several potentially interfering reactions may be identified, and their possible effect must be considered:

$$F + O_2\ (+M) \rightarrow FO_2\ (+M) \quad (14)$$

$$F + CH_3OCH_2 \rightarrow \text{products} \quad (15)$$

$$F + CH_3OCH_2O_2 \rightarrow \text{products} \quad (16)$$

$$CH_3OCH_2 + CH_3OCH_2O_2 \rightarrow \text{products} \quad (17)$$

Reaction 14 occurs in competition with reaction 10. Although the rate coefficient for reaction 10 has not been measured, abstraction of H from organic molecules by F atoms occurs very rapidly (e.g. 8×10^{-11} cm^3 molecule^{-1} s^{-1} for CH_4[16]), and by analogy, a value of $k_{10} > 10^{-10}$ cm^3 molecule^{-1} s^{-1} is predicted. Since this is much higher than the value of $k_{14} = 1.9 \times 10^{-13}$ cm^3 molecule^{-1} s^{-1},[17] the influence of reaction 14 will be negligible at the O_2 concentrations employed. The rate coefficients for reactions 15–17 are unknown. To check for the occurrence of these complicating reactions, two sets of experiments were performed in which the dependences of the maximum transient absorption signal at 260 nm on both radiation dose and SF_6 concentration were investigated. The results are shown in Figures 8 and 9. These plots show good linearity, with the exception of data obtained using full radiation dose and SF_6 concentrations greater than 600 Torr. This indicates that, at the lower doses and SF_6 concentrations, the initial concentration of $CH_3OCH_2O_2$ was proportional to the initial yield of F atoms, confirming that the secondary radical–radical reactions 15–17 are of negligible importance under these experimental conditions.

The solid lines in Figures 8 and 9 are linear least squares fits to the data, using doses less than the maximum and SF_6

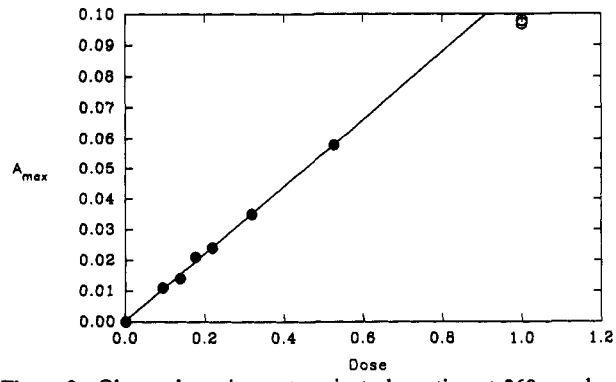

Figure 8. Observed maximum transient absorption at 260 nm due to $CH_3OCH_2O_2$ as a function of radiolysis dose; mixtures were made up of 2.4×10^{16} molecule cm^{-3} CH_3OCH_3, 4.9×10^{17} molecule cm^{-3} O_2, and 2.38×10^{19} molecule cm^{-3} SF_6. The absorption path length was 120 cm.

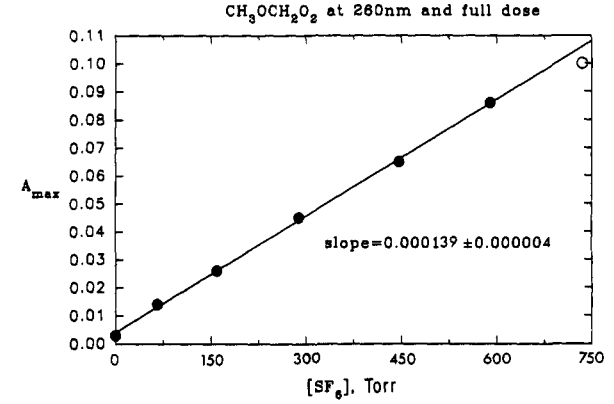

Figure 9. Observed maximum transient absorption at 260 nm due to $CH_3OCH_2O_2$ as a function of $[SF_6]$ at full radiolysis dose; mixtures were made up with 2.4×10^{16} molecule cm^{-3} CH_3OCH_3 and 4.9×10^{17} molecule cm^{-3} O_2. The absorption path length was 120 cm.

concentrations less than 600 Torr. These lines have slopes of 0.109 ± 0.004 units and $(1.39 \pm 0.04) \times 10^{-4}$ $Torr^{-1}$, respectively (errors represent 2σ). From these slopes, the absorbances which correspond to the calibated F atom yield determined above can be calculated, leading to values of $\sigma_{260nm} = (2.01 \pm 0.06) \times 10^{-18}$ and $(1.92 \pm 0.05) \times 10^{-18}$ cm^2 $molecule^{-1}$, respectively. Within the quoted errors, these determinations are in agreement. We choose to quote the average of these values, with error limits which encompass the uncertainty in each determination, $\sigma_{260nm} = (1.97 \pm 0.06) \times 10^{-18}$ cm^2 $molecule^{-1}$. Errors quoted thus far represent the statistical uncertainty associated with the measurements. Incorporating the uncertainty in the absolute calibration of the F atom yield leads to a value of $\sigma_{260nm} = (1.97 \pm 0.21) \times 10^{-18}$ cm^2 $molecule^{-1}$.

To map out the absorption spectrum of $CH_3OCH_2O_2$, experiments were performed to measure the initial absorption at wavelengths between 230 and 300 nm following the pulsed radiolysis of identical $SF_6/CH_3OCH_3/O_2$ mixtures. The observed signals were normalized to the absolute value of σ_{260nm} to obtain the absorption spectrum, which is shown in Figure 6 and Table I along with the spectrum determined using the molecular modulation technique.

Analysis of the observed decay of the absorption at 260 nm using the methods described in previous publications[18,19] provided information on the removal kinetics of $CH_3OCH_2O_2$, initiated by the self reaction. Figure 7 shows a typical transient absorption trace, together with a nonlinear least squares second-order fit. In all experiments, the decay was well described by a second-order analysis. In Figure 10, the reciprocal half-life for the decay of the absorption is plotted as a function of the initial absorption due to $CH_3OCH_2O_2$, for a series of experiments. These data give a value of $k_{5obs}/\sigma_{260nm} = (2.61 \pm 0.10) \times 10^5$ cm s^{-1}, which corresponds to $k_{5obs} = (5.15 \pm 0.58) \times 10^{-12}$ cm^3 $molecule^{-1}$ s^{-1},

TABLE I: UV Absorption Cross Sections Measured for $CH_3OCH_2O_2$ Using the Molecular Modulation (MM) and Pulse Radiolysis (PR) Techniques[a]

wavelength (nm)	MM $10^{18}\sigma$ (cm^2 $molecule^{-1}$)	PR $10^{18}\sigma$ (cm^2 $molecule^{-1}$)
200	2.53	
210	3.61	
220	3.87	
230	3.98	4.06
240	3.72	3.40
250	2.89	2.68
260	2.19	1.97
270	1.40	1.41
280	0.87	0.90
290	0.40	0.49

[a] Uncertainties in determinations at reference wavelengths are $\sigma_{240} = (3.72 \pm 0.41) \times 10^{-18}$ and $\sigma_{260} = (1.97 \pm 0.21) \times 10^{-18}$ cm^2 $molecule^{-1}$ for MM and PR experiments, respectively.

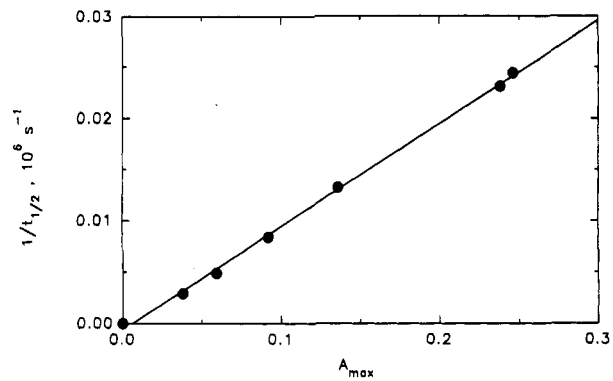

Figure 10. Reciprocal half-life for the decay of absorption due to $CH_3OCH_2O_2$ at 260 nm, plotted as a function of the initial (i.e. maximum) absorption.

using the value of σ_{260nm} determined above. The quoted error was calculated using a propagation of error analysis and incorporates uncertainties in both k_{5obs}/σ_{260nm} and σ_{260nm}.

Variation of the total pressure in the range 75–750 Torr had no significant effect on the measured value of k_{5obs}, which is consistent with the results of the molecular modulation study. The absolute value of k_{5obs}, however, is a factor of 1.5 greater than the maximum value determined at high pressure and high $[O_2]/[Cl_2]$ in the molecular modulation experiments. This discrepancy significantly exceeds the experimental uncertainties in the individual measurements, once again suggesting complications as a result of the secondary chemistry. In particular, the possible effect of the generation of H atoms in the system needs to be considered. In the pulse radiolysis experiments, the concentration of O_2 is necessarily kept low to preclude possible interferences from reaction 14, as discussed above. Furthermore, since the concentration of $CH_3OCH_2O_2$ is high (e.g. about 10^3 times greater than that in the molecular modulation experiments), the reaction of H atoms directly with $CH_3OCH_2O_2$ may be able to compete with the association reaction with O_2:

$$CH_3OCH_2O\ (+M) \rightarrow CH_3OCHO + H\ (+M) \quad (6)$$

$$H + CH_3OCH_2O_2 \rightarrow OH + CH_3OCH_2O \quad (18)$$

$$H + O_2\ (+M) \rightarrow HO_2\ (+M) \quad (11)$$

Reactions 6 and 18 constitute a rapid cycle removing $CH_3OCH_2O_2$, with CH_3OCH_2O and H acting as catalysts:

$$CH_3OCH_2O_2 \rightarrow OH + CH_3OCHO \quad [(6) + (18)]$$

By analogy with the reaction of H with HO_2,[15] reaction 18 would be expected to have a rate coefficient on the order of 10^{-10} cm^3 $molecule^{-1}$ s^{-1}, indicating that reactions 11 and 18 are likely to be competitive under the experimental conditions. Thus, some additional removal of $CH_3OCH_2O_2$ by the cycle (6) + (18) may

TABLE II: Product Yields[a] (%) following the Irradiation of $CH_3OCH_3/Cl_2/N_2/O_2$ Mixtures at a Constant Pressure of 700 Torr

experiment no.	$[O_2]^b$	$[Cl_2]_0{}^b$	Φ-(CH_3OCHO)[c]	Φ-(CH_3OCH_2OOH)[c]
1	3.3×10^0 (0.1)	0.88 (0.027)	91 ± 8	11 ± 2
2	9.8×10^0 (0.3)	3.50 (0.107)	75 ± 21	10 ± 3
3	3.3×10^1 (1.0)	3.37 (0.103)	63 ± 5	14 ± 4
4	3.3×10^2 (10)	3.40 (0.104)	63 ± 2	26 ± 2
5	4.9×10^3 (150)	3.40 (0.104)	63 ± 2	27 ± 2
6	2.3×10^4 (700)	3.37 (0.103)	60 ± 2	28 ± 2

[a] Molar yields relative to CH_3OCH_3 loss, corrected both for the formation of CH_3OCH_2Cl and for secondary reaction with Cl atoms (see text). [b] Concentration in units of 10^{15} molecule cm^{-3} (Torr in parentheses). [c] Quoted errors are 2 standard deviations.

indeed occur. Further complications may arise from the production of OH which either removes further $CH_3OCH_2O_2$ by direct reaction or regenerates $CH_3OCH_2O_2$ by reacting with the precursor CH_3OCH_3 (reactions 1 and 2). Although it is not possible to quantify the effects of these reactions at present, it is clear that k_{5obs} may be significantly enhanced to values greater than $(1 + \alpha)k_5$ as a direct result of the production of H atoms in the system.

3.2. Product Analysis by Long Path Length FTIR Spectroscopy. To obtain complementary information on the mechanism of the self reaction of $CH_3OCH_2O_2$, the stable products of the oxidation of CH_3OCH_3 under a variety of experimental conditions were investigated, using a $Cl_2/CH_3OCH_3/O_2/N_2$ system. The experimental conditions and observed product yields are given in Tables II and III. In each experiment, the reaction mixture was subjected to three to six successive irradiations, each having a duration of 1–20 s. After each irradiation, the reaction mixture was analyzed using FTIR spectroscopy.

Relative Rate Studies for Cl Atom Reactions. In product studies of the Cl atom initiated oxidation of organic compounds, it is important to assess the potential for consumption of the products by secondary reaction with Cl atoms. In the present work, CH_3OCHO, CH_3OCH_2OOH, CH_3OCH_2Cl, HCHO, HCOOH, and CO were detected as products. The reactivities of CH_3OCHO, CH_3OCH_2OOH, HCHO, HCOOH, and CO with Cl have been measured previously.[20-22] There are, however, no available kinetic measurements of the reaction of Cl atoms with CH_3OCH_2Cl. Consequently, preliminary relative rate studies of both this reaction and the reaction of Cl with the reagent CH_3OCH_3 were performed:

$$Cl + CH_3OCH_3 \rightarrow CH_3OCH_2 + HCl \quad (8)$$

$$Cl + CH_3OCH_2Cl \rightarrow \text{products} \quad (19)$$

The experimental techniques employed have been described previously.[12] The rate of reaction 8 was measured relative to that of the reaction of Cl with C_2H_4 (reaction 20), and that of reaction 19, relative to those of both reactions 8 and 20:

$$Cl + C_2H_4 \rightarrow \text{products} \quad (20)$$

Experiments were performed at 700-Torr total pressure. Air diluent was used in the study of the reactivity of CH_3OCH_2Cl relative to CH_3OCH_3. In the other cases, experiments for each reagent/reference pair were performed in both air and N_2 diluents. The results obtained in both diluents were indistinguishable. Representative results are shown in Figure 11. Linear least squares analysis of these data and analogous plots gives the following rate coefficient ratios: $k_8/k_{20} = 2.03 \pm 0.07$; $k_{19}/k_8 = 0.147 \pm 0.005$; and $k_{19}/k_{20} = 0.310 \pm 0.016$. The measured rate coefficient ratios can be placed on an absolute basis using the literature values of the reference rate coefficient, $k_{20} = 9.3 \times 10^{-11}$ cm^3 molecule^{-1} s^{-1}.[23] Hence we derive $k_8 = (1.9 \pm 0.1) \times 10^{-10}$ cm^3 molecule^{-1} s^{-1} and $k_{19} = (2.9 \pm 0.2) \times 10^{-11}$ cm^3 molecule^{-1} s^{-1}. The measured rate coefficient ratio k_{19}/k_8 serves as a cross-check on the measured values of k_{19}/k_{20} and k_8/k_{20}. The consistency is excellent. The measured value of k_8 is in good agreement with previous studies.[24,25] To the best of our knowledge, there have been no previous studies of k_{19}.

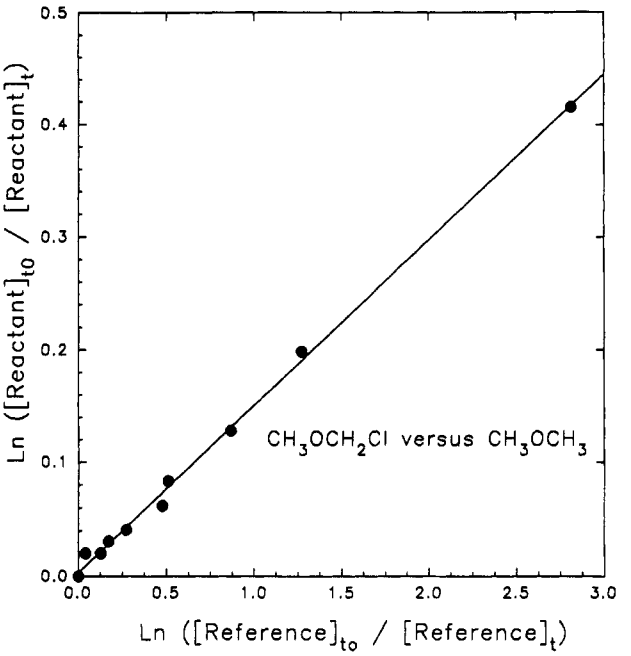

Figure 11. Decay of CH_3OCH_2Cl vs CH_3OCH_3 due to reaction with Cl atoms in relative rate studies.

The above rate coefficients and those measured previously for the reactions of CH_3OCHO, CH_3OCH_2OOH, HCHO, HCOOH, and CO with Cl[20-22] were used to assess the importance of their secondary removal in the study of the oxidation of CH_3OCH_3. Of all the products, CH_3OCH_2OOH and HCHO are the most reactive toward Cl atoms. Even for these species, however, the reactivities are 2–3 times lower than that of CH_3OCH_3. Since only low fractional conversions of CH_3OCH_3 into total products (3–32%) were used, the secondary attack of Cl was not a major complication. Nevertheless, corrections were made using available rate data. These corrections were in the range 0–3% and have been applied to the data presented in Tables II and III.

Product Yields at 700 Torr Total Pressure. Initial experiments were carried out at a total pressure of 700 Torr and with high

TABLE III: Product Yields[a] (%) as a Function of Total Pressure following the Irradiation of $CH_3OCH_3/Cl_2/N_2/O_2$ Mixtures at a Constant O_2 Concentration of 3.3×10^{17} molecule cm^{-3} (10 Torr)

experiment no.	total pressure[b]	$[Cl_2]_0{}^c$	Φ-(CH_3OCHO)[d]	Φ-(CH_3OCH_2OOH)[d]	Φ-(HCHO)[d]	Φ-(HCOOH)[d]	Φ-(CO)[d]
7	10	3.33	43 ± 2	15 ± 2	56 ± 9	4 ± 1	7 ± 1
8	20	3.33	53 ± 2	16 ± 2	46 ± 4	4 ± 1	5 ± 1
9	50	3.57	61 ± 5	17 ± 3	23 ± 2	3 ± 1	2 ± 1
10	100	3.33	62 ± 2	21 ± 2	13 ± 1		
11	300	3.27	64 ± 4	28 ± 4	9 ± 4		
14	700	3.40	63 ± 2	26 ± 2			

[a] Molar yields relative to CH_3OCH_3 loss, corrected both for the formation of CH_3OCH_2Cl and for secondary reaction with Cl atoms (see text). [b] Pressure in units of Torr, with balance N_2. [c] Concentration in units of 10^{15} molecule cm^{-3}. [d] Quoted errors are 2 standard deviations.

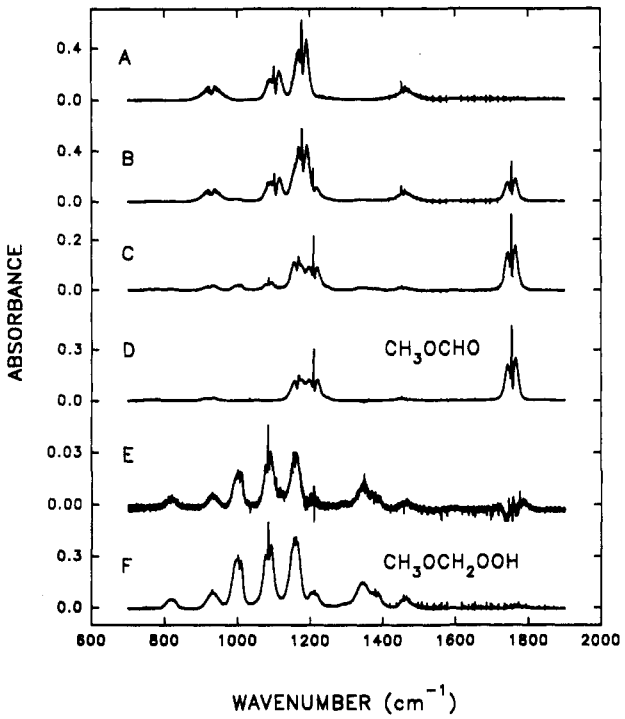

Figure 12. IR spectra acquired before (A) and after (B) 25-s irradiation of a mixture of 9.91×10^{14} molecule cm^{-3} CH_3OCH_3 and 3.37×10^{15} molecule cm^{-3} Cl_2 in 700-Torr O_2 diluent (experiment no. 6). Subtraction of CH_3OCH_3 features from spectrum B gives spectrum C. Reference spectra of CH_3OCHO and CH_3OCH_2OOH are given in spectra D and F. Subtraction of the CH_3OCHO features from spectrum C gives spectrum E. Note the change in y-axis scale.

concentrations of O_2 (5.2×10^{18} and 2.3×10^{19} molecule cm^{-3}) to ensure any H atoms produced in the system reacted exclusively with O_2. Figure 12A and B shows typical spectra acquired before and after 25-s irradiation of a mixture of 9.91×10^{14} molecule cm^{-3} CH_3OCH_3 and 3.37×10^{15} molecule cm^{-3} Cl_2 in 700-Torr O_2 diluent (experiment no. 6). Subtraction of the CH_3OCH_3 features from Figure 12B gives spectrum 12C. Comparison of Figure 12C with a reference spectrum of CH_3OCHO shown in Figure 12D identifies this species as a major product. Subtraction of the features attributable to CH_3OCHO from spectrum 12C gives the residual spectrum 12E. Comparison of this spectrum with a reference spectrum of CH_3OCH_2OOH (Figure 12F) shows this species is also a product. The loss of CH_3OCH_3 was 2.03×10^{14} molecule cm^{-3} (20% of the initial concentration), with yields of CH_3OCHO and CH_3OCH_2OOH of 1.18 and 0.52×10^{14} molecule cm^{-3}, respectively. After subtracting features due to CH_3OCH_2OOH from spectrum 12E, the only other observable product was HCl (2.28×10^{14} molecule cm^{-3}). Figure 13 shows the observed yields of CH_3OCHO and CH_3OCH_2OOH plotted versus the loss of CH_3OCH_3 in experiment no. 6 (see Table II for details). Within the experimental uncertainties, the yields were independent of the fraction of CH_3OCH_3 consumed (4–20%). Linear least squares analysis of the data in Figure 13 gives molar yields for CH_3OCHO and CH_3OCH_2OOH of (60 ± 2)% and (28 ± 2)%, respectively, as reported in Table II. The errors quoted in the Table are 2 standard deviations but do not include potential systematic errors associated with uncertainties in the reference spectra, which are estimated to be ±10%. Combining all the data obtained at $[O_2] \geq 3.3 \times 10^{17}$ molecule cm^{-3} and incorporating this uncertainty lead to yields of 0.63 ± 0.07 and 0.27 ± 0.03 for CH_3OCHO and CH_3OCH_2OOH, respectively.

The observed production of CH_3OCHO and CH_3OCH_2OOH may be accounted for by the mechanism postulated to explain the results of the molecular modulation experiments (see Figure 4), initiated by the self reaction of $CH_3OCH_2O_2$:

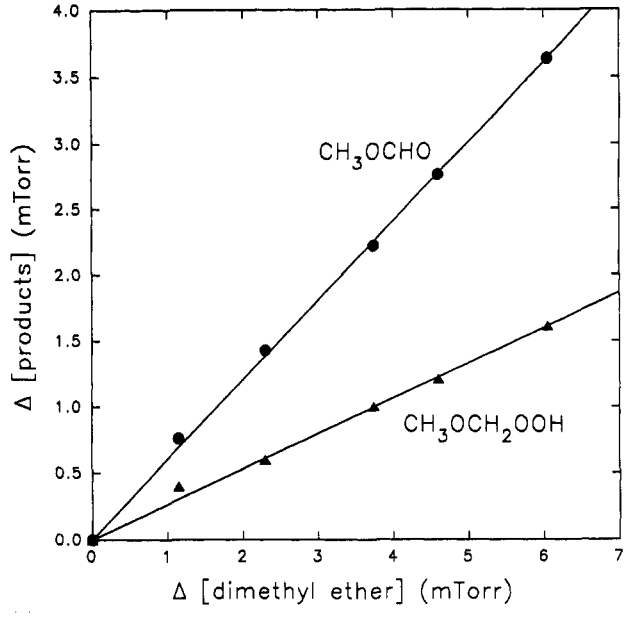

Figure 13. Yields of CH_3OCHO and CH_3OCH_2OOH versus the loss of CH_3OCH_3 observed in experiment no. 6. The solid lines are linear least squares fits.

$$2CH_3OCH_2O_2 \rightarrow 2CH_3OCH_2O + O_2 \quad (5a)$$

$$\rightarrow CH_3OCH + CH_3OCH_2OH + O_2 \quad (5b)$$

$$CH_3OCH_2O\ (+M) \rightarrow CH_3OCHO + H\ (+M) \quad (6)$$

$$H + O_2\ (+M) \rightarrow HO_2\ (+M) \quad (11)$$

$$CH_3OCH_2O + O_2 \rightarrow CH_3OCHO + HO_2 \quad (4)$$

$$HO_2 + CH_3OCH_2O_2 \rightarrow CH_3OCH_2OOH + O_2 \quad (12a)$$

According to this mechanism, CH_3OCHO is formed both directly from the terminating channel 5b and also from the subsequent chemistry of CH_3OCH_2O formed in channel 5a, i.e. either by reaction 4 or reaction 6 followed by (11). These reactions also lead to the quantitative formation of HO_2 and, subsequently, the observed product CH_3OCH_2OOH. On the basis of this chemical scheme, the expected yield of CH_3OCHO relative to CH_3OCH_3 is given by the following expression, where α is the fraction of reaction 5 proceeding by channel 5a:

$$\Phi(CH_3OCHO) = [\alpha + 0.5(1 - \alpha)]/(1 + \alpha) = 0.5 \quad (i)$$

This indicates that the yield of CH_3OCHO should be 0.5, regardless of the value of α, provided HO_2 reacts rapidly to remove additional $CH_3OCH_2O_2$ and this does not produce CH_3OCHO. As indicated above, the measured yield of CH_3OCHO at high O_2 and 700 torr was 0.63 ± 0.07. The fact that this is significantly greater than 0.5 may be explained in two ways. Either the reaction of HO_2 with $CH_3OCH_2O_2$ is sufficiently slow that HO_2 is removed significantly by another route (e.g. self reaction 21) or the reaction occurs rapidly and has a major channel producing CH_3OCHO, reaction 12b:

$$HO_2 + HO_2 \rightarrow H_2O_2 + O_2 \quad (21)$$

$$HO_2 + CH_3OCH_2O_2 \rightarrow CH_3OCHO + H_2O + O_2 \quad (12b)$$

The measurement of the HO_2 steady-state concentration in the molecular modulation experiments was consistent with reaction 12 being both rapid and the dominant removal route for HO_2, and that was implicit in the kinetic analysis (see also the discussion in section 4.2). Therefore, the present result provides evidence for reaction channel 12b. Accordingly, if it is assumed that a fraction β of reaction 12 produces CH_3OCHO, then the yield is given by the following expression:

$$\Phi(CH_3OCHO) = [\alpha(1 + \beta) + 0.5(1 - \alpha)]/(1 + \alpha) \quad (ii)$$

Furthermore, the yield of CH_3OCH_2OOH is given by:

$$\Phi(CH_3OCH_2OOH) = \alpha(1-\beta)/(1+\alpha) \qquad \text{(iii)}$$

Using the measured yields of CH_3OCHO and CH_3OCH_2OOH, 0.63 ± 0.07 and 0.27 ± 0.03, repectively, allows equations ii and iii to be solved simultaneously to obtain the following values of α and β:

$$\alpha = 0.67 \pm 0.13, \beta = 0.33 \pm 0.17$$

The value derived for α agrees very well with the value 0.67 ± 0.11 obtained from the molecular modulation analysis, and the value of β, although approximate, is consistent with a significant contribution of channel 12b to the reaction of HO_2 with $CH_3OCH_2O_2$.

The yields of CH_3OCHO and CH_3OCH_2OOH account for $(90 \pm 8)\%$ of the CH_3OCH_3 removed. According to the above mechanism, the remainder is due to the minor product CH_3OCH_2OH formed in channel 5b. Evidence for the presence of CH_3OCH_2OH was searched for by close examination of the residual spectra in the wavelength region 1000–1200 cm^{-1} where bands due to CH_3OCH_2OH have been reported.[26,27] There were no discernable residual features in this region. On the basis of our previous experience in the FTIR analysis of ethers and alcohols, we assign an upper limit of 15% to the yield of CH_3OCH_2OH.

The effect of varying $[O_2]$ over the range 3.3×10^{15} to 2.3×10^{19} molecule cm^{-3} on the observed product yields was investigated. For most of these studies, the initial concentration of Cl_2 was kept constant at ca. 3.4×10^{15} molecule cm^{-3}, so a range of nearly 4 orders of magnitude variation in $[O_2]/[Cl_2]$ was investigated. The main aim of these experiments was to look for evidence to support the H atom ejection mechanism by allowing the reaction of H with Cl_2 to compete with the reaction with O_2:

$$H + Cl_2 \rightarrow Cl + HCl \qquad (13)$$

$$H + O_2 (+M) \rightarrow HO_2 (+M) \qquad (11)$$

At low $[O_2]/[Cl_2]$ an additional complication arises, however, owing to the reaction of CH_3OCH_2 with Cl_2 competing with the formation of $CH_3OCH_2O_2$:

$$CH_3OCH_2 + Cl_2 \rightarrow CH_3OCH_2Cl + Cl \qquad (22)$$

$$CH_3OCH_2 + O_2 (+M) \rightarrow CH_3OCH_2O_2 (+M) \qquad (2)$$

The influence of the formation of CH_3OCH_2Cl by reaction 22 on the present studies clearly needs to be considered. Since the reaction also returns Cl atoms to the system, which react to regenerate CH_3OCH_2 (reaction 8), this complication was of no significance in the time-resolved molecular modulation experiments reported above:

$$Cl + CH_3OCH_3 \rightarrow CH_3OCH_2 + HCl \qquad (8)$$

This is because the reaction chain (22) + (8) only serves to delay the eventual complete conversion of Cl into $CH_3OCH_2O_2$ by a few milliseconds, without influencing its yield. Although the chain depletes both Cl_2 and CH_3OCH_3, this only occurs to a small extent on the time scale of the molecular modulation experiments. However, the conversion of CH_3OCH_3 into CH_3OCH_2Cl as a result of this "side mechanism" must be taken into account in the analysis of the yields of the stable products.

At partial pressures of O_2 below 100 Torr, CH_3OCH_2Cl was detected as a product. Its yield progressively increased as the $[O_2]/[Cl_2]$ ratio was decreased, indicative of the competition between reactions 2 and 22. At the lowest $[O_2]/[Cl_2]$ (experiment nos. 1 and 2), the yield of CH_3OCH_2Cl accounted for $(73 \pm 3)\%$ and $(69 \pm 4)\%$, respectively, of the CH_3OCH_3 lost. From a consideration of the variation of CH_3OCH_2Cl yield with $[O_2]/[Cl_2]$, we derive an estimate of $k_2/k_{22} = 0.15 \pm 0.05$ at 700-Torr total pressure. In order to determine the product yields resulting from the self reaction of $CH_3OCH_2O_2$, correction for the formation of CH_3OCH_2Cl was necessary. Thus, under conditions

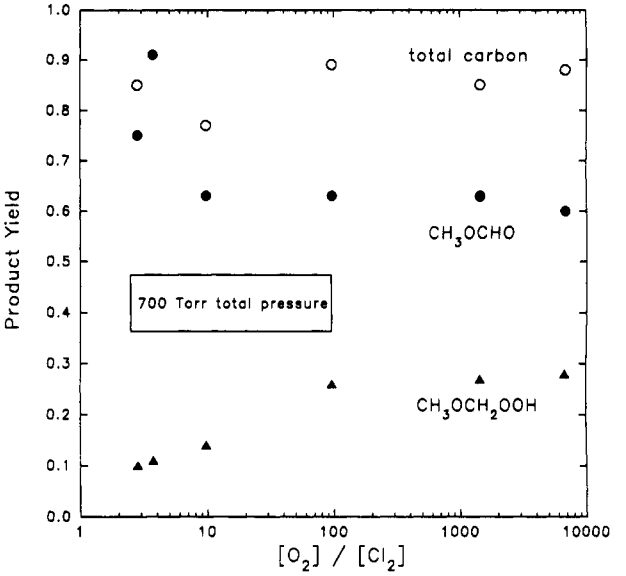

Figure 14. Molar yields of CH_3OCHO (●) and CH_3OCH_2OOH (▲) together with the carbon balance (○) observed following the irradiation of $Cl_2/CH_3OCH_3/O_2/N_2$ mixtures as a function of the concentration ratio $[O_2]/[Cl_2]_0$. The total pressure was held fixed at 700 Torr by the addition of appropriate amounts of N_2 diluent. The yields were calculated using the expression [product]/([CH_3OCH_3] – [CH_3OCH_2Cl]) to account for CH_3OCH_2Cl formation. Small corrections (0–3%) have been applied to account for secondary reactions of Cl atoms (see text for details).

where CH_3OCH_2Cl was formed, the yields of the other products were determined from the expression [product]/(Δ[CH_3OCH_3] – [CH_3OCH_2Cl]). In correcting for the production of CH_3OCH_2Cl, standard error propagation techniques were used so that the uncertainties quoted in Tables II and III for the other products incorporate uncertainties associated with the quantification of CH_3OCH_2Cl.

The variation of the corrected yields of CH_3OCHO and CH_3OCH_2OOH as a function of $[O_2]$ is shown in Figure 14. No significant effect was observed when $[O_2]$ was varied in the range 700–10 Torr. At lower concentrations, when reactions 11 and 13 become competitive, a progressive increase in the yield of CH_3OCHO is observed at the expense of CH_3OCH_2OOH. In the limit, when $[O_2]/[Cl_2]$ is sufficiently low that H reacts exclusively with Cl_2, HO_2 should no longer be produced in the system by reaction 9, and the formation of CH_3OCH_2OOH should be totally suppressed. The corresponding limiting yield of CH_3OCHO is given by the expression:

$$\Phi(CH_3OCHO) = [0.5(1+\alpha)] \qquad \text{(iv)}$$

Using the value of $\alpha = 0.67 \pm 0.11$ suggests a yield of $\Phi(CH_3OCHO) = 0.84 \pm 0.06$, with the remaining loss of CH_3OCH_3 due to CH_3OCH_2OH formation. This is in good agreement with the yield of CH_3OCHO observed at the lowest $[O_2]/[Cl_2]$ studied (Figure 14).

The only other product detected at 700-Torr total pressure was HCl. At high $[O_2]/[Cl_2]$ ratios (experiment no. 5), the yield of HCl relative to CH_3OCH_3 lost was found to be 1.1 ± 0.1, which is consistent with its production solely from reaction 8:

$$Cl + CH_3OCH_3 \rightarrow CH_3OCH_2 + HCl \qquad (8)$$

At low $[O_2]/[Cl_2]$ (experiment no. 1), the observed yield of HCl, 1.6 ± 0.2, is significantly greater than unity, giving strong evidence of an additional source of HCl resulting from the presence of H atoms in the system:

$$H + Cl_2 \rightarrow Cl + HCl \qquad (13)$$

Clearly the measured product yields and their dependence on $[O_2]/[Cl_2]$ at 700-Torr total pressure are entirely consistent with

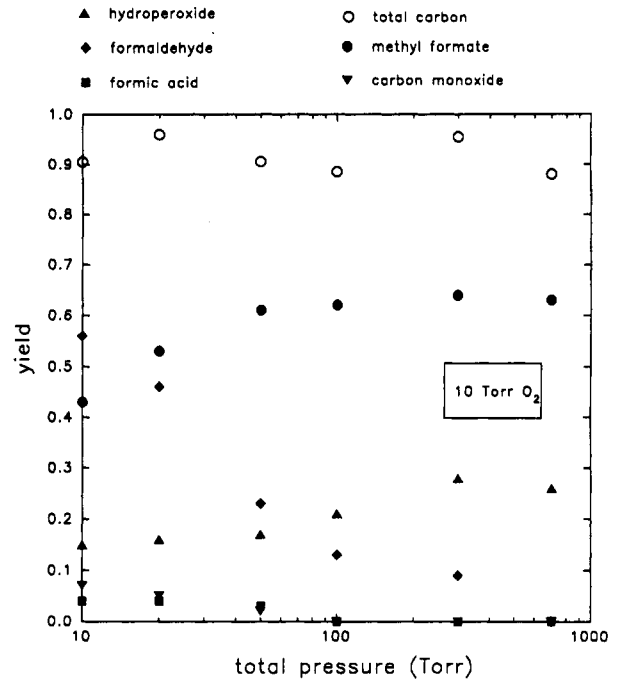

Figure 15. Molar yields of CH_3OCHO (●), CH_3OCH_2OOH (▲), HCHO (◆), HCOOH (■), and CO (▼) together with the carbon balance (○) observed following the irradiation of $Cl_2/CH_3OCH_3/O_2/N_2$ mixtures as a function of total pressure with the concentration ratio $[O_2]/[Cl_2]_0$ fixed at 98 ± 5. The yields were calculated using the expression [product]/([CH_3OCH_3] – [CH_3OCH_2Cl]) to account for CH_3OCH_2Cl formation. Small corrections (0–3%) have been applied to account for secondary reactions of Cl atoms (see text for details).

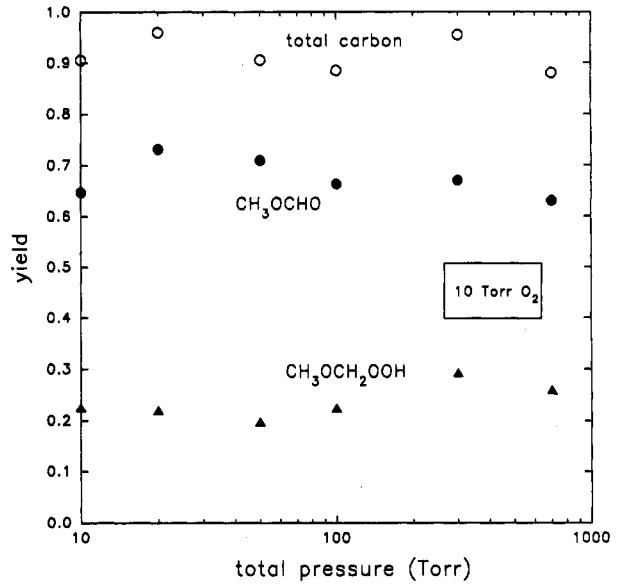

Figure 16. Molar yields of CH_3OCHO (●) and CH_3OCH_2OOH (▲) as a function of pressure, after correction for the formation of HCHO and the minor secondary products, CO and HCOOH, formed from the oxidation of HCHO (see discussion in text).

the mechanism presented in Figure 4, involving the production of H atoms from the thermal decomposition of CH_3OCH_2O.

Product Yields as a Function of Total Pressure. Further experiments were performed as a function of total pressure in the range 10–700 Torr, with $[O_2]$ and $[Cl_2]$ kept constant at ca. 3.3 × 10^{17} and 3.3 × 10^{15} molecule cm^{-3}, respectively. This was primarily to search for evidence for the competition between the pressure-dependent reaction 11 and the pressure-independent reaction 13 for H. In addition to CH_3OCHO and CH_3OCH_2OOH, however, several other carbon-containing products (HCHO, HCOOH, and CO) were detected at lower pressures. The observed product yields are given in Table III and Figure 15. There was no evidence (<2% yield) for these additional products in any of the experiments performed at 700-Torr total pressure, as listed in Table II.

The most significant of these products was HCHO, its formation becoming progressively more important as the pressure was lowered (300–10 Torr). Although a decrease in the yield of the major product CH_3OCHO was also observed at low pressures, possibly indicative of HCHO formation by an alternative decomposition reaction 23 for CH_3OCH_2O and the subsequent reaction 24, we do not believe this process to be important:

$$CH_3OCH_2O\ (+M) \rightarrow CH_3O + HCHO\ (+M) \quad (23)$$

$$CH_3O + O_2 \rightarrow HCHO + HO_2 \quad (24)$$

This is because significant formation of HCHO is detected at pressures ≥50 Torr, although no corresponding reduction in the yield of CH_3OCHO is observed.

An alternative explanation is required in which HCHO is formed by a process occurring in competition with a pressure-dependent reaction. Other than reaction 6, the only pressure-dependent reaction of an organic radical in the proposed scheme is reaction 2. The formation of HCHO might occur if the peroxy radical adduct initially formed in reaction 2, $[CH_3OCH_2O_2]^\dagger$, is able to undergo an isomerization to CH_2OCH_2OOH, followed by decomposition as follows (reaction 2′):

$$CH_3OCH_2 + O_2 \dashrightarrow [CH_3OCH_2O_2]^\dagger \xrightarrow{M} CH_3OCH_2O_2 \quad (2)$$

$$[CH_3OCH_2O_2]^\dagger \dashrightarrow CH_2OCH_2OOH \dashrightarrow 2HCHO + OH \quad (2')$$

Such an isomerization–decomposition could occur via a six-membered transition state, possibly by a concerted mechanism. The OH produced simultaneously with HCHO in reaction 2′ reacts with CH_3OCH_3 to regenerate CH_3OCH_2:

$$OH + CH_3OCH_3 \rightarrow CH_3OCH_2 + H_2O \quad (1)$$

Consequently this mechanism leads to the chain formation of HCHO by reaction sequence (2′) + (1). The chain length increases as the pressure is lowered, since it is only terminated by the stabilization of $[CH_3OCH_2O_2]^\dagger$ occurring in competition with its isomerization. It is important to note that this "side mechanism" does not influence the initial yield of $CH_3OCH_2O_2$ from Cl, which is consistent with the results of the kinetic studies.

If this explanation of the HCHO production is correct, the yields of the major products, CH_3OCHO and CH_3OCH_2OOH, following the self reaction of $CH_3OCH_2O_2$ may only be interpreted if they are corrected for the formation of HCHO by the side chain, in a similar manner to the corrections made for CH_3OCH_2Cl above. Corresponding corrected yields are shown in Figure 16. In contrast to the results obtained by varying $[O_2]/[Cl_2]$ at 700 Torr, the corrected yields of CH_3OCHO and CH_3OCH_2OOH are comparatively insensitive to variation of total pressure. Over the pressure range 700–50 Torr, the CH_3OCH_2OOH yield decreases from 27% to ca. 20%, and the CH_3OCHO yield increases from 63% to 71%. This is consistent with a progressively greater proportion of the H atoms generated in the system reacting with Cl_2, i.e. analogous to that observed when $[O_2]/[Cl_2]$ was decreased at 700-Torr total pressure, as described in the previous section. Over the pressure range 50–10 Torr, however, the yield of CH_3OCHO decreases and the yield of CH_3OCH_2OOH increases so that, at 10 Torr, the high-pressure yields are almost regained. This is consistent with the results of the molecular modulation experiments at 25-Torr pressure, where it was believed that the reaction of CH_3OCH_2O with O_2 was able to compete with the thermal decomposition reaction 6, thereby precluding the formation of H atoms in the system:

$$CH_3OCH_2O\ (+M) \rightarrow CH_3OCHO + H\ (+M) \quad (6)$$

$$CH_3OCH_2O + O_2 \rightarrow CH_3OCHO + HO_2 \quad (4)$$

Under conditions where reaction 4 dominates, the yields of CH_3OCHO and CH_3OCH_2OOH would be expected to be indistinguishable from those observed at high pressure.

The minor products HCOOH and CO were only detected under conditions when significant concentrations of HCHO were generated (see Figure 15) and can be explained by the secondary attack of HO_2 and Cl (or possibly OH) on HCHO. The addition reaction of HO_2 with HCHO leads to the formation of $HOCH_2O_2$, which reacts with itself and HO_2 (and probably $CH_3OCH_2O_2$ in the present system) to generate HCOOH as described in detail previously:[28]

$$HO_2 + HCHO \rightleftarrows HOCH_2O_2 \quad (25)$$

The attack of Cl or OH on HCHO generates CO by the following well-established chemistry:[15]

$$Cl + HCHO \rightarrow HCl + HCO \quad (26)$$

$$OH + HCHO \rightarrow H_2O + HCO \quad (27)$$

$$HCO + O_2 \rightarrow HO_2 + CO \quad (28)$$

4. Discussion

4.1. UV Absorption Spectrum of $CH_3OCH_2O_2$. The UV absorption cross sections measured for $CH_3OCH_2O_2$ in the present study and those reported previously by Dagaut et al.[8] are shown in Figure 6. The present measurements, using two chemical systems and two experimental techniques, agree to within 10% at all common wavelengths other than 290 nm. At this wavelength, where the cross section is about an order of magnitude below its peak value, the two determinations differ by about 20%. The two sets of data are also in excellent agreement with the cross sections reported by Dagaut et al.[8] across the complete wavelength range.

The value of σ at the absorption maximum is ca. 4×10^{-18} cm^2 molecule^{-1}, which is comparable with values typically observed for unsubstituted alkyl peroxy radicals.[3,4] Clearly the presence of the oxygen atom on the carbon adjacent to the chromophore does not have a major influence on the magnitude of the absorption spectrum. In common with the case of other halogen and oxygen α-substituted alkyl peroxy radicals, however, the observed position of the absorption maximum is shifted to shorter wavelength.[3,4] For $CH_3OCH_2O_2$, the electron-withdrawing influence of the oxygen linkage apparently causes a shift of ca. 10 nm compared with the case of $C_2H_5O_2$. In the case of the closely related radical $HOCH_2O_2$, however, the effect is far less obvious, the shift to shorter wavelength being at most 5 nm compared with the case of CH_3O_2. This may be a consequence of some internal hydrogen bonding involving the chromophore causing a competing effect on the position of the maximum. In the case of the β-substituted $HOCH_2CH_2O_2$ radical, where the electron-withdrawing influence of the oxygen linkage is reduced but internal hydrogen bonding still probably occurs, the position of the spectral maximum is ca. 5 nm longer in wavelength than that observed for $C_2H_5O_2$.[3,4]

4.2. Kinetics and Branching Ratio of the Self Reaction of $CH_3OCH_2O_2$. The kinetic experiments presented in section 3.1 indicate that the rate of the self reaction of $CH_3OCH_2O_2$ is insensitive to variation of pressure in the range 17–760 Torr at 298 K:

$$2CH_3OCH_2O_2 \rightarrow 2CH_3OCH_2O + O_2 \quad (5a)$$

$$\rightarrow CH_3OCHO + CH_3OCH_2OH + O_2 \quad (5b)$$

The dependence of the apparent rate coefficient, k_{5obs}, on both pressure and the composition of the reaction mixtures observed in the present work, and previously by Dagaut et al.,[8] is believed to occur as a direct result of the formation of H atoms in the system from the thermal decomposition of CH_3OCH_2O (produced in channel 5a), which will be discussed below. The observed kinetics under conditions where the secondary chemistry resulted in further removal of $CH_3OCH_2O_2$ provided a value of $(1 + \alpha)k_5 \approx 3.5 \times 10^{-12}$ cm^3 molecule^{-1} s^{-1} at 298 K. This is in reasonable agreement with the corresponding high-pressure limiting value (2.7×10^{-12} cm^3 molecule^{-1} s^{-1}), which can be calculated for 298 K from the optimized falloff expression given by Dagaut et al.[8]

The molecular modulation experiments and the FTIR product analysis provided values of α of 0.67 ± 0.11 and 0.67 ± 0.13, respectively, and a value of $k_5 = (2.13 \pm 0.30) \times 10^{-12}$ cm^3 molecule^{-1} s^{-1} for the elementary rate coefficient. An important assumption in the analyses leading to these parameter values was that HO_2 formed as a result of channel 5a was removed exclusively and rapidly by reaction 12:

$$HO_2 + CH_3OCH_2O_2 \rightarrow \text{products} \quad (12)$$

Using the approximate value of $k_{12} = 10^{-11}$ cm^3 molecule^{-1} s^{-1} and the steady-state concentration ratio $[HO_2]/[RO_2] \approx 0.3$ derived from the UV spectral measurements presented in section 3.1, it can be calculated that reaction 12 accounts for ca. 86% of the removal of HO_2 in the system at 760 Torr, with the self reaction of HO_2 being a minor removal route ($k_{21} = 2.8 \times 10^{-12}$ cm^3 molecule^{-1} s^{-1}):[15]

$$HO_2 + HO_2 \rightarrow H_2O_2 + O_2 \quad (21)$$

Since reaction 12 is the dominant, but not the exclusive, removal route for HO_2, the analyses for α and k_5 are approximate. Furthermore, the lifetime of HO_2 may be sufficiently long that the removal kinetics of $CH_3OCH_2O_2$ are not truly second order. On the basis of the present kinetic measurements, and those reported previously,[8] however, the deviations from second-order behavior are clearly very subtle and well within the experimental noise. Similarly, the errors in the derived values of α and k_5 from using the simplified analysis are also comparatively small. For example, if the minor participation of reaction 21 in the system is allowed for, the values of k_{5obs} measured in the molecular modulation experiments would be expected to vary from $(1 - \alpha)k_5$ at low $[O_2]/[Cl_2]$ to $(1 + 0.86\alpha)k_5$ (rather than $(1 + \alpha)k_5$) at high $[O_2]/[Cl_2]$, leading to revised values of $\alpha = 0.72$ and $k_5 = 2.24 \times 10^{-12}$ cm^3 molecule^{-1} s^{-1}. The differences between these parameters and those derived from the original analysis are significantly lower than the experimental error. In the absence of an independent, direct measurement of the kinetics of reaction 12, therefore, the original assumption is believed to be adequate, and we conclude that $\alpha = 0.7 \pm 0.1$ and $k_5 = (2.1 \pm 0.3) \times 10^{-12}$ cm^3 molecule^{-1} s^{-1}.

The presence of the oxygen linkage adjacent to the peroxy radical center in $CH_3OCH_2O_2$ clearly provides an activating influence, since k_5 is a factor of ca. 30 greater than the self reaction rate coefficient for $C_2H_5O_2$.[3,4] Similarly, the self reaction of $HOCH_2O_2$ is some 15 times more rapid than the self reaction of CH_3O_2 at 298 K.[3,4] The value of α is similar to those observed for a series of primary organic peroxy radicals ($R'CH_2O_2$), which typically lie in the range 0.6–0.7.[3,4]

The FTIR product studies of reaction 5 were complicated at lower pressures by the formation of significant concentrations of HCHO. Other than the proposed isomerization–decomposition mechanism for the reaction of the methoxy methyl radical with O_2, involving a six-membered cyclic transition state (reaction 2′), it is difficult to identify a source of HCHO in the system which is consistent with the experimental observations:

$$CH_3OCH_2 + O_2 \dashrightarrow [CH_3OCH_2O_2]^\dagger \xrightarrow{M} CH_3OCH_2O_2 \quad (2)$$

$$\downarrow$$

$$CH_2OCH_2OOH \dashrightarrow 2HCHO + OH \quad (2')$$

Although speculative, this mechanism is similar to that proposed to account for the formation of carbonyl products and HO_2 from the reactions of a series of α-hydroxy alkyl radicals with O_2 at ambient temperatures.[29-33] In these cases, the isomerization

occurs via a five-membered cyclic transition state, e.g. the reaction of the hydroxy methyl radical with O_2:

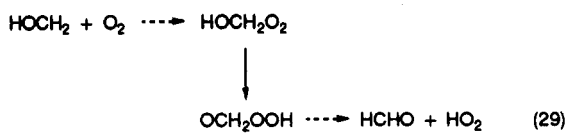

$$HOCH_2 + O_2 \dashrightarrow HOCH_2O_2 \quad OCH_2OOH \dashrightarrow HCHO + HO_2 \qquad (29)$$

Evidence for the occurrence of reaction 2′ was obtained at 300 Torr and below. Clearly further work on the oxidation at lower pressures is required, since the overall effect of reaction 1 followed by reaction 2′ is the OH catalyzed conversion of CH_3OCH_3 into HCHO, which may have significance to the atmospheric degradation of CH_3OCH_3 (and other ethers) in the upper troposphere:

$$CH_3OCH_3 + O_2 \rightarrow 2HCHO + H_2O \qquad [(1) + (2')]$$

In principle, mechanisms analogous to reaction 2′ may also occur for α-alkoxy alkyl peroxy radicals of general formula $R_1R_2CHOC(OO)R_3R_4$. There are, however, no published investigations of any such species at pressures below 700 Torr.

4.3. Thermal Decomposition of α-Alkoxy Alkoxy Radicals. In sections 3.1 and 3.2, evidence from kinetics and product studies was presented which supports a mechanism involving the rapid thermal decomposition of the CH_3OCH_2O radical by H atom ejection, occurring in competition with its reaction with O_2:

$$CH_3OCH_2O\ (+M) \rightarrow CH_3OCHO + H\ (+M) \qquad (6)$$

$$CH_3OCH_2O + O_2 \rightarrow CH_3OCHO + HO_2 \qquad (4)$$

Atkinson and Carter[34] have estimated a heat of formation of CH_3OCH_2O of ca. −148 kJ mol^{-1}, from which $\Delta H \approx 16$ kJ mol^{-1} can be calculated for reaction 6 (i.e. approximately thermoneutral), suggesting that the H atom ejection mechanism is plausible. The corresponding reaction enthalpy for the potential alternative decomposition channel 23, which was rejected as the source of HCHO in the low-pressure product study, is 57 kJ mol^{-1}.

$$CH_3OCH_2O\ (+M) \rightarrow CH_3O + HCHO\ (+M) \qquad (23)$$

It is interesting to note that Veyret et al.[35] obtained evidence for a thermal dissociation pathway analogous to reaction 6 for the closely related radical, $HOCH_2O$:

$$HOCH_2O\ (+M) \rightarrow HCOOH + H\ (+M) \qquad (30)$$

They derived the expression $k_{30} = 10^{14} \exp(-7500/T)$ from experiments performed at low total pressures, which corresponds to ca. 1200 s^{-1} at 298 K. The present data suggest that reactions 4 and 6 are competitive at 25 Torr, with $[O_2]$ in the range (1–6) $\times 10^{17}$ molecule cm^{-3}. If k_4 is assumed to occur at 10^{-14} cm^3 molecule^{-1} s^{-1} (i.e. typical for reactions of alkoxy radicals with O_2), with reactions 4 and 6 proceeding at equal rates at the center of this $[O_2]$ range, a value of k_6 of ca. 3000 s^{-1} may be calculated. Thus, we conclude that H atom ejection from CH_3OCH_2O and $HOCH_2O$ occurs at comparable rates. Although it is likely that reactions 4 and 6 are also competitive at 760 Torr and higher $[O_2]$ ($>10^{18}$ molecule cm^{-3}), when both reactions occur more rapidly, no information on the competition could be obtained at this pressure. Consequently, both reactions 4 and 6 may occur under tropospheric conditions. Like reaction 30, reaction 6 will be strongly dependent on temperature.

Wallington and Japar[36] have established that the α-alkoxy alkoxy radicals formed in the degradation of diethyl ether and ethyl *tert*-butyl ether predominantly eject a CH_3 group in preference to reaction with O_2 (R = C_2H_5, $(CH_3)_3C$):

$$ROCH(O)CH_3\ (+M) \rightarrow ROCHO + CH_3\ (+M) \qquad (31)$$

Apparently there is a strong driving force for the formation of formate esters from the reactions of α-alkoxy alkoxy radicals. In the case of alkoxy methoxy radicals such as $(CH_3)_3COCH_2O$ formed from methyl *tert*-butyl ether (a widely used fuel additive), this may involve ejection of an H atom. Under tropospheric conditions, however, the sole fate of the H atom is reaction with O_2 to produce HO_2 (reaction 11), leading to the same overall products as if the alkoxy methoxy radical had reacted with O_2. Thus we recommend that the tropospheric behavior of alkoxy methoxy radicals is adequately represented by the reaction:

$$ROCH_2O + O_2 \rightarrow ROCHO + HO_2 \qquad (32)$$

Acknowledgment. M.E.J. and G.D.H. gratefully acknowledge support from the Commission of the European Communities (under Contract EV4V-0082-C) and the Natural Environment Research Council (under Contract F3/G12/31).

References and Notes

(1) Calvert, J. G.; Madronich, S. *J. Geophys. Res.* **1987**, *92*, 2211.
(2) Atkinson, R. *Atmos. Environ. A* **1990**, *24*, 1.
(3) Lightfoot, P. D.; Cox, R. A.; Crowley, J. N.; Destriau, M.; Hayman, G. D.; Jenkin, M. E.; Moortgat, G. K.; Zabel, F. *Atmos. Environ. A* **1992**, *26*, 1805.
(4) Wallington, T. J.; Dagaut, P.; Kurylo, M. J. *Chem. Rev.* **1992**, *92*, 667.
(5) Japar, S. M.; Wallington, T. J.; Richert, J. F. O.; Ball, J. C. *Int. J. Chem. Kinet.* **1990**, *22*, 1257.
(6) Carter, W. L.; Atkinson, R. *J. Atmos. Chem.* **1985**, *3*, 377.
(7) Jenkin, M. E. Ph.D. Thesis, University of East Anglia, Norwich, U.K., 1991.
(8) Dagaut, P.; Wallington, T. J.; Kurylo, M. J. *J. Photochem. Photobiol.* **1989**, *48*, 187.
(9) (a) Jenkin, M. E.; Cox, R. A. *J. Phys. Chem.* **1985**, *89*, 192. (b) Jenkin, M. E.; Cox, R. A.; Hayman, G. D.; Whyte, L. J. *J. Chem. Soc., Faraday Trans. 2* **1988**, *84*, 913.
(10) Hansen, K. B.; Wilbrandt, R.; Pagsberg, P. *Rev. Sci. Instrum.* **1979**, *50*, 1532.
(11) Nielsen, O. J. Risø Report R-480, 1984.
(12) Wallington, T. J.; Gierczak, C. A.; Ball, J. C.; Japar, S. M. *Int. J. Chem. Kinet.* **1989**, *21*, 1077.
(13) Seery, D. J.; Britton, D. *J. Phys. Chem.* **1964**, *68*, 2263.
(14) Meister, M.; Swick, G.; Griesbaum, K. *Can. J. Chem.* **1983**, *61*, 2385.
(15) Atkinson, R.; Baulch, D. L.; Cox, R. A.; Hampson, R. F.; Kerr, J. A.; Troe, J. *J. Phys. Chem. Ref. Data* **1992**, *21*, 1125.
(16) Wallington, T. J.; Maricq, M. M.; Ellermann, T.; Nielsen, O. J. *J. Phys. Chem.* **1992**, *96*, 982.
(17) Ellermann, T.; Sehested, J.; Nielsen, O. J.; Pagsberg, P.; Wallington, T. J. *Chem. Phys. Lett.*, submitted.
(18) Kurylo, M. J.; Ouellette, P. A.; Laufer, P. H. *J. Phys. Chem.* **1986**, *90*, 437.
(19) Sander, S. P.; Watson, R. T. *J. Phys. Chem.* **1981**, *85*, 2960.
(20) Wallington, T. J.; Hurley, M. D.; Ball, J. C.; Jenkin, M. E. *Chem. Phys. Lett.* **1993**, *211*, 41.
(21) Demore, W. B.; Sander, S. P.; Golden, D. M.; Hampson, R. F.; Kurylo, M. J.; Howard, C. J.; Ravishankara, A. R.; Kolb, C. E.; Molina, M. J. Jet Propulsion Laboratory Publication 92–20, Pasedena, Ca, 1992.
(22) Wallington, T. J.; Andino, J. M.; Ball, J. C.; Japar, S. M. *J. Atmos. Chem.* **1990**, *10*, 301.
(23) Wallington, T. J.; Andino, J. M.; Lorkovic, I. M.; Kaiser, E. W. *J. Phys. Chem.* **1990**, *94*, 3644.
(24) Michael, J. V.; Nava, D. F.; Payne, W. A.; Stief, L. J. *J. Chem. Phys.* **1979**, *70*, 3652.
(25) Wallington, T. J.; Skewes, L. M.; Siegl, W. O.; Wu, C. H.; Japar, S. M. *Int. J. Chem. Kinet.* **1988**, *20*, 867.
(26) Silverman, D. G.; Freeman, J. J. *Ind. Eng. Chem. Process Des. Dev.* **1983**, *22*, 441.
(27) Johnson, R. A.; Stanley, A. E. *Appl. Spectrosc.* **1991**, *45*, 218.
(28) Burrows, J. P.; Moortgat, G. K.; Tyndall, G. S.; Cox, R. A.; Jenkin, M. E.; Hayman, G. D.; Veyret, B. *J. Phys. Chem.* **1989**, *93*, 2374.
(29) Grotheer, H. H.; Riekert, G.; Walter, D.; Just, T. *J. Phys. Chem.* **1988**, *92*, 4028.
(30) Nesbitt, F. L.; Payne, W. A.; Stief, L. J. *J. Phys. Chem.* **1988**, *92*, 4030.
(31) Pagsberg, P.; Munk, J.; Anastasi, C.; Simpson, V. J. *J. Phys. Chem.* **1989**, *93*, 5162.
(32) Miyoshi, A.; Matsui, H.; Washida, N. *Chem. Phys. Lett.* **1989**, *160*, 291.
(33) Miyoshi, A.; Matsui, H.; Washida, N. *J. Phys. Chem.* **1990**, *94*, 3016.
(34) Atkinson, R.; Carter, W. L. *J. Atmos. Chem.* **1991**, *13*, 195.
(35) Veyret, B.; Roussel, P.; Lesclaux, R. *Int. J. Chem. Kinet.* **1984**, *16*, 1599.
(36) Wallington, T. J.; Japar, S. M. *Environ. Sci. Technol.* **1991**, *25*, 410.